INVITED PAPER

# Propagation Issues for Cognitive Radio

*While the CR system designer can determine the transmit power, it is the propagation channel that determines how much of that power arrives as interference to primary and other CR users.*

By Andreas F. Molisch, *Fellow IEEE*, Larry J. Greenstein, *Life Fellow IEEE*, and Mansoor Shafi, *Fellow IEEE*

**ABSTRACT** | Cognitive radios are expected to work in bands below about 3.5 GHz and may be used for a variety of applications, e.g., broadband fixed wireless access, mobile and nomadic access, etc. Cognitive radio system designers must have access to a wide range of channel models covering a wide span of operating frequencies, carrier bandwidths, deployment conditions, and environments. This paper provides a comprehensive overview of the propagation channel models that will be used for the design of cognitive radio systems. We start with classical models for signal loss versus distance and discuss their dependence on the physical properties of the environment and operating frequency. Here we also introduce the concept of log-normal shadowing resulting from signal blockage by man-made and natural features. Next, we discuss the time-varying nature of the wireless channel, introduced as a result of the motion of objects in the channel. This is followed by a discussion on the dispersion of the signal caused by various effects of propagation, especially in the time and frequency domains. Angular dispersion, which is discussed next, is important because cognitive radios may be based on modems that exploit the spatial domain. Lastly, we summarize channel models that have been standardized for fixed and mobile systems.

**KEYWORDS** | Angle-of-arrival; channel models; delay spread; dispersion; Doppler; multipath propagation; path loss; shadowing

Manuscript received January 14, 2009. First published April 24, 2009; current version published May 1, 2009.

**A. F. Molisch** is with the Department of Electrical Engineering at the University of Southern California, Los Angeles, CA 90089 USA (e-mail: Andreas.Molisch@ieee.org).
**L. J. Greenstein** is with Rutgers University-WINLAB, North Brunswick, NJ 08902 USA (e-mail: ljg@winlab.rutgers.edu).
**M. Shafi** is with Telecom New Zealand, Wellington, New Zealand.

Digital Object Identifier: 10.1109/JPROC.2009.2015704

## I. INTRODUCTION

Cognitive radio (CR) is a term for radios that are aware of their surroundings and adapt their transmission parameters (including, but not limited to, carrier frequency and bandwidth) to the environment and the interference situation. In the words of [1]: "Cognitive radio is an intelligent wireless communication system that is aware of its surrounding environment (i.e., outside world), and uses the methodology of understanding-by-building to learn from the environment and adapt its internal states to statistical variations in the incoming RF stimuli by making corresponding changes in certain operating parameters (e.g., transmit-power, carrier-frequency, and modulation strategy) in real-time, with two primary objectives in mind: (i) highly reliable communications whenever and wherever needed; (ii) efficient utilization of the radio spectrum."

The fundamental principle of CR is thus to identify other radios in the environment that might use the same spectral resources, and to then design a transmission strategy that minimizes interference to and from those radios. For the identification, design, implementation, and analysis of transmission strategies, it is essential to understand the propagation *channel*. The power emitted by a transmitter (TX) might be determined by the system designer, but it is the channel that determines how much of it arrives as useful power at the intended receiver (RX), and also how much interference is created at a victim receiver. The time variations of the channel response determine how often potential interference levels have to be estimated and, thus, how often transmission strategies may have to be adapted. As we will see, many other properties of the channel influence CR design and analysis as well. First, however, we present here some high-level information about CR bands, wireless channels, and the relationship between them.

CRs may be deployed over a wide range of the frequency spectrum. The bands below about 3.5 GHz have lower propagation loss and are sought after by all services. These bands are therefore ideal candidates for the deployment of CR. They have different incumbent (primary) systems, each with its own mix of service type, architecture, bandwidth, and resilience to interference. Some typical candidate bands for CR systems are as follows.

- *UHF bands:* These bands are currently used by broadcast television, though some conversion to wireless broadband services is in progress. Terrestrial broadcasting transmitters tend to have high antennas (hundreds of meters) and large powers (kilowatt range). In this service, the transmission is one-way, the transmitting antenna may be outside the area containing the CRs, and the TV customers are generally fixed. The U.S. regulatory body, the Federal Communications Commission, has recently adopted rules to allow unlicensed radio transmitters to operate in the broadcast television spectrum at locations where the spectrum is not being used by the licensed services. The unused TV spectrum is often termed "white spaces." This might be one of the first spectrum ranges where innovative products and services using CR systems may appear.
- *Cellular bands:* Typical cellular bands are centered near 800/900 MHz, 1.8/1.9 GHz, 2.1 GHz, 2.3 GHz, and 2.5 GHz. IMT-Advanced systems [fourth-generation cellular systems as defined by the International Telecommunications Union (ITU)] may also be deployed in the 3.5 GHz band. Cellular networks have ubiquitous coverage, with cell site antennas mounted typically at rooftop or lamp post height. This service is two-way, with the cell sites generally in the same region as the CRs, and the cellular customers can be mobile.
- *Fixed wireless access bands:* These bands provide two-way broadband services and are centered near 2.5 and 3.5 GHz. Fixed wireless systems are similar in layout to cellular networks, with the customers at fixed locations, like homes and businesses.

In these and most other bands, wireless signals are affected by the propagation in a number of ways. They undergo attenuation, the local spatial average of which—expressed in decibels—is called the path loss. This is a large-scale property of the channel, in that it changes mildly over distances of a great many wavelengths. There is also a small-scale variation of signal level, for a given value of path loss, which is due to the presence of multiple signal paths; this is called *multipath fading* and is characterized by rapid fluctuations in signal level over distances of a radio wavelength. The multiple paths arise from scattering, reflection, and diffraction related to objects and structures in the physical environment and can lead to serious signal distortion.

The properties of wireless channels can vary with carrier frequency and service bandwidth. For example, large-scale properties like the path loss tend to increase linearly with the logarithm of the carrier frequency [2]; by contrast, small-scale properties like the signal distortion are relatively insensitive to carrier frequency but their effect can depend a lot on the service bandwidth. All of this pertains to both cognitive and primary radios, and so both radio types require good channel models to enable effective designs.

Here, we provide an overview of the propagation models that might be used by CR system designers and researchers. These models can help to determine, via analysis or simulation, potential CR interference to primary systems; and they can dictate the design of transmission formats, routing algorithms, and control schemes for mitigating interference from CRs. Moreover, because the spectrum acquired for CR use may span a wide and fragmented range, propagation models are needed for a wide variety of frequencies and bandwidths. We stress that the physical propagation channel is independent of whether the radio is cognitive or not. However, the issues of what aspects of the channel are important, and thus have to be modeled especially carefully, are different. In particular, the special feature of CR—and the main motivation for this paper—is the strong potential of interference to primary users. This makes the availability of good channel models even more imperative.

In Section II, we elaborate on the above discussion with a brief overview of CR and the impact of propagation. Section III discusses the nature and modeling of large-scale channel properties such as path loss and shadow fading. Section IV does the same for small-scale channel properties such as fading statistics and the Ricean $K$-factor. Models for the delay, frequency, and angle dispersions of wireless channels are covered in in Sections V–VII. In Section VIII, we briefly discuss the dependencies of those different types of dispersion. Section IX cites key references for the values of model parameters, as used by industry practitioners. Section X discusses, in conclusion, typical uses of channel models in the analysis and design of CR systems.

## II. OVERVIEW OF COGNITIVE RADIO

### A. Cognitive Radio Systems

In general, a *cognitive radio* adapts to the current state of the environment, including the spectrum usage [1], [3], [4]. There are actually two different definitions for cognitive radio.

- A *spectrum-agile cognitive radio,* which only adapts the center frequency, bandwidth, and transmission time according to the environment. Such a cognitive radio approach is also often called *dynamic spectrum access*.

- A *fully cognitive radio,* which adapts all transmission parameters to the environment, i.e., modulation format, multiple-access method, coding, as well as center frequency, bandwidth, transmission times, and so on.

In the following, we will mainly discuss spectrum-agile CRs, as they have larger practical importance at this time and in the foreseeable future. At the same time, we will also briefly discuss channel characteristics as they impact fully-cognitive radios.

A key motivation for the use of CR comes from the fact that spectrum is not exploited to its full extent at all times [5]. If, for example, no active users are present in a cell of a cellular system, the spectrum is unused in this particular area. Similarly, a lot of the spectrum assigned to TV transmission is not used. Regulatory environments for CR can be classified as follows [6].

- *Dynamic exclusive model:* Here, a frequency band is still reserved for the exclusive use of a particular service, but different providers can share the spectrum.
- *Open sharing model:* Here, all users can access the spectrum equally, subject to certain constraints on the characteristics of the transmit signal. Such an approach is used today, for example, in the industrial, medical, and scientific bands.
- *Hierarchical access model:* This model assigns different priorities to different users. Primary users should be served in such a way that they experience the same service quality as if the spectrum were reserved exclusively for their usage. Secondary users are allowed to transmit, but only in such a way that they do not (or only "insignificantly") affect the performance or service quality of the primary users. The secondary users adaptively decide whether they might use parts of a spectrum that is assigned by default to primary users.

In order to simplify notation, all our subsequent examples refer to the hierarchical access model, though our qualitative considerations about the impact of propagation channels on the CR design and performance hold for the other regulatory environments as well.

To reiterate, the key principle of hierarchical CR is that the secondary users do not disturb the primary users. Such nondisturbance can be achieved by three fundamental approaches: *interweaving, overlay, and underlay* [4], [6], [7].

- In an *interweaving* system, a secondary user tries to identify and transmit in spectral white space, i.e., at the times/locations/frequencies where primary users are not active. The secondary system thus first has to perform spectrum sensing, which usually is done as energy detection, i.e., determining whether the energy observed by the secondary user can be explained by noise energy alone or whether it indicates the presence of a primary signal. It is noteworthy that a secondary system usually can only sense the presence of a primary TX, not that of an RX; the impact of this fact will be discussed below.
- In an *overlay* approach, the secondary system identifies the propagation channel from both the primary and the secondary transmitters to the primary receiver. The secondary system then uses its knowledge of the propagation channels to make sure that the secondary transmission does not reduce the quality of the primary transmission, even when secondary and primary transmission occur in the same frequency band. Overlay usually requires knowledge of the complex impulse response (transfer function) over the relevant transmit–receive paths (e.g., between primary and secondary transceivers), and is thus more complicated than the sensing task of interweaving.
- In an *underlay* approach, the secondary transmitter keeps its transmit power spectral density at such a low level that the primary receiver sees only a slight enhancement of its effective noise level, even though the transmit spectrum of the secondary signal might overlap with that of the primary system. Ultra-wide-band (UWB) communications are a classical example of underlay.

### B. Impact of Propagation on Sensing

The energy-sensing process is influenced in a myriad of ways by the propagation channel.

- The signal level at a sensor (part of the secondary system) is determined by the path loss (Section III) of the link between this sensor and the primary transmitter, as well as by the large-scale (Section III) and small-scale (Section IV) fading of this link. The signal level, in turn, influences the tradeoff between the false-alarm probability (spectrum is declared occupied even though it is free) and the missed-detection probability (spectrum is declared empty even though it is occupied by a primary user).
- When wide-band sensing is used, the signal levels are different at different frequencies, due to the frequency selectivity of small-scale fading (Section V), as well as possibly through the frequency dependence of the path loss (Section III). Knowledge of these effects is essential for building appropriate wide-band sensors (e.g., [8]).
- When distributed sensing is used, knowledge of the correlation of the channel characteristics from the primary transmitter to the sensors is required. Such knowledge includes the path-loss laws and correlation statistics of the shadowing (Section III).
- When antenna arrays are used for sensing, the angular spread (Section VII) determines the correlation of the signals at the different antenna elements, and thus the optimum detection process.

- Further improvements of the detection process can be achieved when sensing data are averaged over time. In order to perform proper averaging, the secondary system needs to know both the transmission statistics of the primary system and the temporal variability of the channel (Section VI).

As we mentioned above, a sensor usually can only detect the presence of a primary transmitter, not of a receiver. It is nontrivial to draw conclusions from these observations about whether transmission from secondary devices create excessive interference to a primary receiver. Imagine as a simple scenario a primary system using frequency-domain duplexing. Then each primary receiver also acts as transmitter, but in a different band. It is then essential to understand the correlation of the signal levels in the transmit and receive bands of the primary system (this is related to the frequency selectivity of the small-scale fading and the frequency dependence of the path loss).

Propagation channels also have a key influence on the "hidden node problem," where a secondary transceiver is outside the "listening range" for a primary transmitter but close enough to the primary receiver to create interference. The likelihood for hidden nodes to occur increases with increasing path loss and shadowing variance.

### C. Impact of Propagation Channels on Transmission Strategy

After sensing, the next step for the secondary system is to find a good transmission strategy. In the case of a spectrum-sensing radio (i.e., just changing the operating frequency), this involves a decision about which secondary transmitter can transmit in which frequency band, and for how long. In other words, the "free" spectrum has to be distributed among the different secondary devices that want to transmit information. Optimum assignment strategies can often be obtained from game-theoretic considerations [9]. As an input to such computations, knowledge of the propagation channels is essential. The actual performance as well as the relative effectiveness of different schemes depends on the observed signal levels. For an overlay approach (see, e.g., [10]), the secondary system needs accurate knowledge of the propagation channel from the primary receiver to both the primary and secondary transmitter at the time of actual transmission. In order to develop proper transmission strategies, it is vital that the secondary transmitter be able to make channel predictions (based on the past and present observations) and that it understand the achievable accuracy of those predictions. This, in turn, requires good channel models.

The necessity of updates in the optimum transmission scheme is intimately tied to the temporal properties of the channel, including the Doppler spectrum for mobile users (Section III-B) and temporal variations (Section III-C) of the Rice factor for fixed users. This also has an impact on whether cooperative games or noncooperative games can be used to develop a transmission strategy. Cooperative games require exchange of information between the different secondary users, but if the channel changes too rapidly (large Doppler spread) and/or too strongly (small temporal Rice factor), the overhead for the required information exchange becomes too large.

The channel characteristics also have an impact on the design of the transmission strategy for CRs. For example, the optimum subcarrier spacing in orthogonal frequency-division multiplexing depends on the power delay profile and the Doppler spectrum [11]. Thus, a CR should adjust its subcarrier spacing to the propagation channel. The size of the modulation alphabet should be adapted to the signal level (which depends on path loss, shadowing, and small-scale fading). As a general rule, we can say that every single operating parameter in a CR depends in some way on the propagation channel.

## III. PATH-LOSS MODELS

### A. Background

The most important aspect of any characterization of radio propagation is how field strength varies as a function of distance and location. This property is usually captured in the concept of *path loss*. It is defined as the decibel (dB) value of the ratio of the transmitted power to the received power. In this definition, the value used for received power is a spatial average over the local area, as we will explain later. Path loss is a fundamental mechanism that ensures that a CR TX will not disturb a primary receiver if it is far enough away.

Given the path loss, along with the transmitted power and the antenna gains at each end of a radio path, the analyst/designer can determine how much power is received (on average) from a particular TX. Typically, one might want the aggregate of the powers received from interfering transmitters to be at least 10 dB lower than that received from the desired transmitter. For any given application, the threshold value may be lower or higher than 10 dB, depending on the specifics of the radio design.

There are many published models of path loss that pertain to the frequency bands and types of locales in which CRs may operate [2], [12]–[19]. Many textbooks [11], [20]–[23] have described the various mechanisms that enable us to describe signal attenuation. At the same time, there have been extensive measurement campaigns over the years that model path loss in specific frequency bands and environments; the corresponding list of papers and reports is very long but see, for example, [2], [12], [13], [24], and [25].

The simplest path-loss model is that for free-space propagation. This applies when there is a direct line-of-sight (LOS) path from transmitter to receiver and no

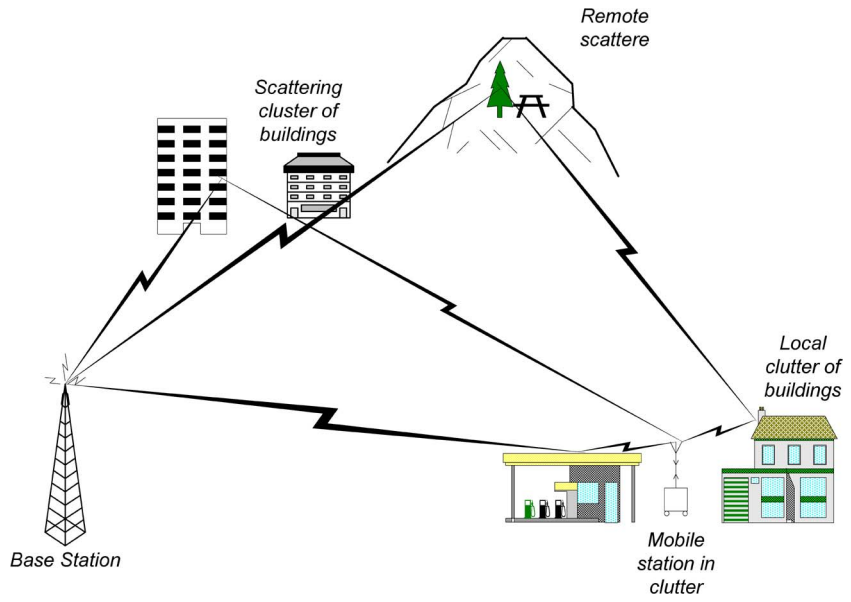


**Fig. 1.** ***Principle of multipath propagation.***

obstructions, reflections, or scatterings. In this case, the path loss is

$$\mathrm{PL} = 32.4 + 20\log_{10}(f d_{\mathrm{km}})\mathrm{dB} \tag{1}$$

where $f$ is the frequency in megahertz and $d_{\mathrm{km}}$ is the path length (distance) in km. Thus, for example, the free-space path loss at 1 GHz and 1 km is 92.4 dB.

### B. Received Power

Usually, radio paths in wireless systems do not at all meet the free-space conditions. There is often no LOS term, and the non-LOS (NLOS) paths are numerous due to multiple obstructions, reflections, and scattering that make up the received signal; see Fig. 1. We now present a generic description of received power on wireless paths that will aid us in subsequent discussions. It is

$$p_r = p_t\left[a\left(\frac{d}{d_0}\right)^{-\gamma}\zeta s\right] \tag{2}$$

where $p_r$ and transmit power $p_t$ are in consistent units; $a$ is a constant that can depend on frequency, antenna heights, and other factors; $d$ and $d_0$ are path length and a reference distance, respectively, in consistent units; $\gamma$ is the so-called path-loss exponent; and $\zeta$ and $s$ represent "small-scale" and "large-scale" fading, respectively, which we explain next.

*1) Small-Scale and Large-Scale Fading:* The factor $\zeta$ varies spatially, i.e., if the receiver moves even slightly from some starting point, the received power can change significantly. This is because, in a multipath environment (meaning one in which the transmitted signal takes multiple paths to the receiver), the received signal's complex amplitude is the sum of multiple vectors whose relative phases change with receiver position. Thus, for example, the net magnitude of the received signal can change significantly over a half-wavelength of travel; at an operating frequency of 2 GHz, this amounts to just 7.5 cm. The variation of received signal magnitude over such short distances is called small-scale fading (it is also called *multipath fading* to describe its cause); and $\zeta$, which represents this fading, is usually normalized so that its local spatial average is one. Thus, the local spatial average of the received power $\langle p_r \rangle$ is (2) with $\zeta$ replaced by one. We model small-scale fading in Section IV.

The factor $s$ also varies spatially, but it has a different cause and a considerably larger spatial scale. It reflects the fact that the locally averaged received power does not depend solely on distance but also on the particular structures along the path, especially obstructing objects such as hills and buildings. Thus, the distance-dependent part of (2) accounts for much of the influence on received power, but there is also a variation about that part, and it is represented by $s$. This factor changes over distances of tens to hundreds of meters, i.e., a scale typical of the sizes of city blocks or neighborhoods. It is called large-scale fading, in contrast to the small-scale fading due to multipath, and is also called *shadow fading* to describe its frequent cause—the shadowing produced by obstructions on the path. Typically, $s$ is normalized so that its median value is one. Thus, the local spatial average of $p_r$ has a *median* value over the environment given by (2), but with $\zeta$ and $s$ replaced by one. We model large-scale fading in Section III-C.

Small-scale and large-scale fading also play an important role in the design of CR radios by introducing randomness into the received power. If fading did not exist, then a CR could compute the power received at the primary and secondary RXs purely from the geographical locations of the transceivers (which, in turn, could be derived from the power received at known anchor nodes or GPS receivers, or by other means). Due to the small-scale and large-scale fading, knowledge of the distance to the TX does not allow unique conclusions about the received (useful or interference) power. The magnitude of the power variations is clearly an important factor in the computation of interference probability. The spatial and temporal scales over which the variations occur have an impact on how a channel has to be sensed, how far apart sensing nodes need to be located so that the fading at them can be considered uncorrelated, and how probable a "hidden node" is. For example, a CR receiver might sense that a channel is available because small-scale fading leads to a strong attenuation from a primary TX/RX. If the CR then transmits a little bit later, when the attenuation has changed due to the small-scale fading, the radiation emitted by the CR will lead to a high interference power.

*2) Path Loss:* Let us assume, for the moment, that the antennas at both ends of a transmit–receive path are omnidirectional (radiating equally in all directions), in which case the term $a$ in (2) depends only on the nature of the environment, not on the antennas. In that case, we can call the quantity $\langle p_r \rangle / p_t = (a(d/d_0)^{-\gamma} s)$ the *path loss* and $(a(d/d_0)^{-\gamma})$ the *median path loss*. These quantities are properties solely of the path geometry and the environment surrounding the path. Their dB values lead us to formal descriptions of path loss and median path loss. We discuss antenna gains later.

Following convention, we define path loss (PL) to be the negative of the dB value of the path gain, i.e.,

$$\mathrm{PL} = -10 \log_{10}\left(\frac{\langle p_r \rangle}{p_t}\right) = \left[A + 10\gamma \log_{10}\left(\frac{d}{d_0}\right)\right] + S \quad (3)$$

where $A$ and $S$ are the negative dB values of $a$ and $s$, respectively. This generic form is common to most path-loss models, some of which contain "break points" in distance $d$ where the value of $\gamma$ changes. In a number of published treatments, moreover, "path loss" is defined as the bracketed term in (3), with shadow fading, $S$, treated separately. We take the alternative approach, wherein "path loss" is the sum of the shadow fading and the bracketed term, and we call the latter the *median* path loss.

There are more complex expressions of path loss that are based on empirical measurements. These expressions relate the path loss to the heights of TX and RX, frequency of operation, distance, and environment type (e.g., urban, suburban, etc.). Reference [2] gives the path-loss expressions for 900/1800 MHz, [104] has those for 2.1 GHz, and [25] has measurements and models for carrier frequencies around 5 GHz.

### C. Shadow Fading Model

Measurements over the years have demonstrated that $s$ in (2) has a log-normal distribution over space, meaning that $S$ in (3) has a Gaussian distribution over space. Specifically, $S$ can be modeled as a two-dimensional Gaussian process over space with zero mean and a standard deviation $\sigma$.

Whereas this describes the first-order statistics of shadow fading, which is well supported by data [14], [19], [21], the second-order statistics of shadow fading, i.e., its autocorrelation function over space, are far less documented. A widely used model is due to Gudmundson [26], although other measurements have also been reported, e.g., [27]. The model in [26] treats the correlation of $S$ between two points separated by distance $\Delta x$ as

$$\langle S(x) S(x + \Delta x) \rangle = \sigma^2 \exp\left(-\frac{|\Delta x|}{X_c}\right) \quad (4)$$

where $X_c$ is the so-called correlation distance of shadow fading. Typical values of $X_c$ range from 10 m (i.e., in urban microcells) to 500 m (i.e., in some urban macrocells). The value of $\sigma$ also takes on a range of values, from as low as 3 dB in some indoor environments to as much as 12 dB in some outdoor macrocells. The value most generally used in cellular and fixed wireless macrocells is 8 dB.

### D. Median Path-Loss Model

Many papers and reports have been published on the median path loss, e.g., [2] and [12]–[14]. What distinguishes one set of authors from another is how they model the parameters $A$ and $\gamma$. We now describe one approach in depth. In this and subsequent descriptions, our purpose is not to prescribe recipes to be followed by all users but, rather, to illustrate by concrete example the nature of channel models for wireless environments.

The model in [14] is derived from 1.9 GHz data collected over 95 macrocells in suburban environments, with the user terminal at a height of 2 m. The data span a variety of base-station antenna heights and terrain types, and the model includes their impact. Extensions to other frequency bands and user terminal heights could be made using simple scaling laws, (e.g., as in [19]) or by collecting new data and applying a similar methodology. The model for median path loss from [14] is as follows.

- Up to the reference distance $d_0$ (which is taken to be 100 m), the median path loss follows the free-space path-loss formula, whereby $A = 20 \log_{10}(4\pi d_0/\lambda)$, with $\lambda$ the wavelength at the center frequency and $\gamma = 2$. For a center frequency of 1.9 GHz, $A = 78.0$ dB.

- For $d > d_0$, $A$ remains the same but $\gamma$ is a quantity that varies randomly from one macrocell to another. Over all cells, it has a mean value $\mu_\gamma$ that depends on the base-station antenna height $h_b$ and on the terrain type; and a zero-mean variable part whose standard deviation $\sigma_\mu$ depends on the terrain type only.
- Specifically, $\mu_\gamma = (a - bh_b + (c/h_b))$, where $h_b$ is in meters; $(a, b, c)$ are constants determined by terrain type, in units that make $\mu_\gamma$ dimensionless; and this formula applies for $h_b$ from 10 to 80 m.
- The variable part of $\gamma$ is represented using a truncated Gaussian probability distribution, the truncation being chosen to preclude $\gamma$ from ever going negative.

We note that [14] also treats the shadow fading parameter $\sigma$ as changing randomly from one cell to another, the variation being represented by a truncated Gaussian distribution. The numerical values of this model ($a, b, c, \sigma_\gamma$, etc.), are summarized in [14, Table 1] for each of three broad terrain categories. The model thus incorporates the randomness of the model from one cell to another, the influence of terrain type, and the influence of base-station antenna height.

The scaling of median path loss for frequency is implicit in the cited formula for $A$, since $\lambda$ is inversely proportional to frequency $f$. Thus, it might be concluded that the path loss grows as $20\log_{10} f$, a relationship known in radio as the antenna aperture effect. To account for diffraction around obstructing objects on the path, an effect that weakens with increasing $f$, [19] suggests that PL for this model be augmented by an added decibel term $6\log_{10}(f/2000)$, where $f$ is in megahertz. It also suggests an added decibel term proportional to $-\log_{10}(h_t/2)$, where terminal antenna height $h_t$ is in meters and the proportionality constant depends on the terrain type. This added term adjusts for the effect of terminal antenna heights other than 2 m.

### E. Antenna Gain and the Gain Reduction Factor

Antennas are never truly omnidirectional. In cellular base stations, for example, the antennas have gain in the elevation plane in order to focus the antenna beam on the ground area containing user terminals; and they may have moderate azimuth gains (beamwidths between 60° and 120°) to improve reuse efficiency through *sectoring*. If the gain of the transmit antenna towards a receiver is $G_t$ dB and the gain of the receive antenna towards the transmitter is $G_r$ dB, then the path gain will be augmented, in theory, by an amount $(G_t + G_r)$ dB. This gain can produces a significant benefit against noise.

The notion of an antenna with a highly directive beam and correspondingly low antenna side-lobes suggests a potential benefit for a CR receiver: by pointing such a beam at its intended transmitter, it can both improve its received signal level and suppress interfering signals coming from off-beam directions. Some fixed wireless systems have also considered directive beams, for the same reason. (This approach is most feasible to contemplate when the link ends are not moving.) Nonetheless, propagation studies conducted in this context showed that, in the presence of wide-angle scatter, the benefits of high directivity will not necessarily be realized.

Based on an extensive data collection, a model was devised for the amount by which directive gain is reduced by multipath scatter [28]. The main finding was that substantial gain reductions occur with high probability in typical wireless environments. The amount of gain reduction—whose dB value is called the *gain reduction factor* (GRF)—is a random variable from one path to another. The model for GRF in suburban residential environments, as reported in [28] and standardized in [19], is as follows.

- GRF is a lognormal random variable whose natural logarithm has a mean $\mu_{\text{grf}}$ and a standard deviation $\sigma_{\text{grf}}$.
- $\mu_{\text{grf}} = -(0.53 + 0.1I)\ln(\beta/360) + (0.5 + 0.04I)(\ln(\beta/360)^2)$, where $I = 1$ for winter and $-1$ for summer; and $\beta$ is the directive antenna beamwidth in degrees.
- $\sigma_{\text{grf}} = -(0.93 + 0.02I)\ln(\beta/360)$.

The practical effect of this model, in the kinds of environments where CRs often operate, is this: both the gain in the direction of the intended (CR) transmitter and the side-lobe suppression in the directions of unwanted interferers are often severely mitigated by wide-angle scatter, thereby diminishing the hoped-for benefit of using directive CR antennas. For example, an antenna with a 30° beamwidth and a gain of about 11 dB loses all but 4 dB all of that gain with 50% probability. For antennas with even higher directivity (and gain), the reductions are even greater. More detailed information on the angular distributions of arriving echoes is given in Section VII.

## IV. SMALL-SCALE FADING AND THE RICEAN K-FACTOR

### A. Spatial Variation of Field Strength

As we have noted, the electric field strength fluctuates rapidly over space if there is a lot of multipath, as in typical wireless environments. This is because the field at a particular point is the sum of several components, each with a magnitude and phase, and each phase changes from one point to another (by 360° in a distance equal to the wavelength $\lambda$). More important, the relative phases of the components change, so that the net magnitude and phase of the sum varies. This variation over space is what we call either small-scale fading or multipath fading, as we discussed in Section III.

If the field were sampled at many points within a radius of, say, $10\lambda$, we would obtain a population of many magnitudes whose values are describable using a *probability density function* (pdf), and the same is true of the phase.

The most common and widely understood situation is the one where all the multipath components are of similar magnitude so that, in the central limit of a great many components, their sum has a variation over space that resembles a complex Gaussian process. It has been shown that the phase of a complex Gaussian random variable has a uniform pdf over $(-\pi, \pi]$; and that the magnitude has a *Rayleigh* pdf [11], [21]. This case is thus referred to as *Rayleigh fading*. Since the power received by an antenna at a given point in space is proportional to the squared magnitude of the field strength, the received power in Rayleigh fading has a decaying exponential for its pdf. For this case, the dynamic range between the first and ninety-ninth percentiles is 26.6 dB. This signifies a great deal of fading of received signal from one point on the terrain to another.

In some cases, there is a dominant term among the many arriving components, i.e., one whose magnitude is much higher than all others. This happens, for example, when there is a direct ray (LOS path) from the transmitter to the receiver. In this case, the vector sum of all arriving component magnitudes has a pdf called *Ricean*, which is characterized by two parameters: i) the power of the dominant component $p_d$ and ii) the local spatial average of the power sum of all the weaker (scatter) terms $p_s$. A more popular but equivalent parameter pair is the total spatial average of received power $p_d + p_s$ and the ratio $p_d/p_s$. The former parameter can be recognized as the average received power $\langle p_r \rangle$, discussed in the previous section. The latter parameter is called the *Ricean K-factor* or *Rice-factor*, or just $K$. It is a measure of how much local fading the signal undergoes over space. When $K$ is infinite, there is no fading (only a single component, e.g., an LOS term, as in free space) and when $K = 0$ ($-\infty$ dB), there is Rayleigh fading as described above (no dominant component, only scatter).

We note that, for an LOS component, the magnitude does not change rapidly over space but the phase does, while the scatter component changes rapidly in both magnitude and phase. Also, we emphasize that the local average of received power is closely related to the path loss PL. Assuming omnidirectional antennas at both ends of the wireless link, we can write $\langle p_r \rangle$ as simply $p_t 10^{-0.1\mathrm{PL}}$ so that modeling path loss and $K$ are sufficient for characterizing the pdf of small-scale fading. The $K$-factor varies with distance. Measurements at 5 GHz and using 100 MHz carrier bandwidths have produced the following model for the distance dependence of the dB value of $K$ [25]:

$$K(\mathrm{dB}) = \begin{cases} 8.7 + 0.051d & \text{Indoor Environments} \\ 3.7 + 0.019d & \text{Rural Environments} \\ 3.0 + 0.014d & \text{Urban Microcells.} \end{cases} \quad (5)$$

An alternative model for the Ricean $K$ is described in [29]. Here $K$ is modeled as a lognormal random variable whose mean is distance dependent; this dependence, as well as variance and autocorrelation, are specified in [29].

### B. Temporal Fading on Mobile Radio Links

So far we have discussed signal fading as a random variation over space, i.e., over potential receiver locations on the ground. What translates this spatial process into a *temporal* process is the fact that a mobile terminal moves over the ground, and as it does it will experience fading, in time, of its received signal strength. Thus, the Rayleigh/Ricean fading descriptions given above materialize as temporal processes in mobile operation. The higher the speed of the mobile, the more rapid is the fading.

Therefore, it is also important to characterize the statistics of the random fading over time, i.e., to model the *second-order statistics* of fading. This is captured in the power density spectrum of the fading, commonly called the *Doppler spectrum*. The name relates to the fact that multipath components (see Fig. 1) arriving from different angles have different Doppler shifts, so the composite received signal has a distribution of power over frequency, one that depends on the distribution of received power over arrival angle. This idea will be further elaborated in Section VI. Here, we merely note that the Doppler spectrum (and its inverse Fourier transform, the *fading autocorrelation function*) are additional aspects of small-scale fading that must be addressed.

### C. Temporal Fading on Fixed Wireless Links

The notion of temporal fading on a fixed wireless path may seem strange at first because we have been explaining it as a random time variation of the signal level received by a mobile terminal. We recall that fading arises from the presence of many received *multipath components* (MPCs), each with a phase that is highly sensitive to both antenna position and signal frequency (or wavelength). The result is that the net received signal magnitude is a random-looking function of both position and frequency. In a mobile terminal, it is the variation over space that produces the temporal fading of the received signal. In fixed wireless, the two ends of a link are nonmoving, so whereas the "fading" over frequency can be discerned, one would not expect to see temporal fading. That such fading exists nonetheless leads us to a different way of thinking about, and modeling, the Ricean $K$-factor.

In a mobile link, a mobile "traces out" the spatial fading as it moves, the scaling factor between distance traveled and time elapsed being the mobile speed $v$. Thus, if $E(x)$ is the field variation along the mobile direction $x$, then the temporal variation is just $E(vt)$. In a fixed wireless link, the variation is due instead to the fact that some scattering objects are moving—a prime example being windblown leaves and limbs of trees. In fixed wireless systems operating in suburban residential areas, trees can be a large factor in producing temporal fading of received signal strength. Moving cars and people can have a similar impact in wireless ad hoc networks and wireless local-area networks.

Extensive measurements reported in [30], covering many frequencies, observation times, and paths, and several locales within the United States, produced the following findings.

1) Temporal fading on fixed wireless links can be characterized by Ricean distributions.
2) The Ricean $K$-factor shows a significant variation from one observation time, frequency, and path to another.
3) The rate of fading is generally related to the prevailing wind speed.

In this case, the fixed scatterers produce the constant term in the complex magnitude and the moving scatterers produce the variable term. The ability to represent temporal fading as Ricean is fortunate, again, because it involves only two parameters (path loss and $K$-factor), and also because it permits the use of analysis methods similar to those developed for mobile radio.

The model for Ricean $K$-factor on fixed wireless paths has been standardized in [19], based largely on [30] but also corroborated by data in [31]. It can be described as follows.

- The $K$-factor can be expressed as a random variable

$$K = F_s F_h F_b K_0 d^{\gamma} u \tag{6}$$

  where $K_0 = 10$; $\gamma = -0.5$; $d$ is transmitter–receiver distance in kilometers; $u$ is a log-normal variable whose dB value has a mean of zero and standard deviation of 8.0 dB; and $F_s$, $F_h$, and $F_b$ are factors that account for season, user terminal height, and base antenna beamwidth, respectively.
- $F_s = 1.0$ in summer (leaves on trees) and $F_s = 2.5$ in winter (no leaves).
- $F_h = (h/3)^{0.46}$, where $h$ is the height of the user antenna, in meters.
- $F_b = (b/17)^{-0.62}$, where $b$ is the base antenna beamwidth, in degrees.

This model applies to paths from fixed wireless TXs into fixed CR receivers and helps to quantify the amount of variation of fixed wireless interference power. Low $K$-factors (which, the model predicts, occur quite often) can lead to periods of very low interference power (deep fades). Whether such fades can be exploited by CR receivers depends on the fade durations, which again relates to the Doppler spectrum of fading. As discussed later, this spectrum for fixed wireless fading is very different from the Doppler spectrum for mobile fading (see Section VI).

## V. DELAY DISPERSION

As we discussed in Section III, a signal sent out from the TX can travel to the RX via different paths that might involve reflection, diffraction, or scattering. Thus, multiple echoes (MPCs) of the original signal arrive at the RX, which have different delays, directions, and frequency (Doppler) shifts. Multipath propagation leads to *dispersion* in the delay, angle, and Doppler domain, which can also be interpreted as *selectivity* in the frequency, space, and time domains. In this and the following two sections we discuss this dispersion and its impact on the design and performance of CRs. We start by discussing delay- and frequency-dispersion only, since this is the situation most relevant for TXs and RXs with only one (omnidirectional) antenna. We then extend the discussion to directional dispersion, which impacts cognitive radio systems with directional antennas, and in particular can be exploited by cognitive systems that can perform adaptive beamforming.

### A. Time-Variant Channel Impulse Response

Let us take a closer look at the detailed properties of these MPCs. Each MPC might cover a different total distance and thus require different amounts of runtime (distance divided by speed of light) to get from the TX to the RX. An RX that simply collects all arriving signals (i.e., an RX with an omnidirectional antenna) therefore receives multiple copies of the signal that are delayed with respect to each other. Furthermore, each of those signal copies is attenuated and phase shifted on its path, and noise is present as well. The total received signal is thus

$$r(t) = \sum_{i=1}^{L} a_i(t) s(t - \tau_i) + n(t) \tag{7}$$

where $a_i(t)$ is the time-varying complex amplitude of the $i$th MPC, $s(t)$ and $r(t)$ are the transmit and receive signal, respectively, and $n(t)$ is a noise signal, commonly modeled as additive white Gaussian noise. Note that the transmit signal depends on time, but that also the complex attenuation coefficient of the MPCs depends on time. We assume here that the attenuation coefficient changes very slowly compared to the duration of the signal (e.g., the symbol duration in a digital transmission) and the delays of the MPCs—an assumption that is true for almost all practical systems. We can also describe the received signal as the convolution of the transmit signal with the time-variant impulse response (i.e., the output of the channel if the transmit signal is a very short pulse), which is

$$h(t, \tau) = \sum_{i=1}^{L} a_i(t) \delta(\tau - \tau_i). \tag{8}$$

Note that this impulse response is time-variant: at different absolute times $t$, a different impulse response $h(\tau)$ characterizes the channel. The actual value of this

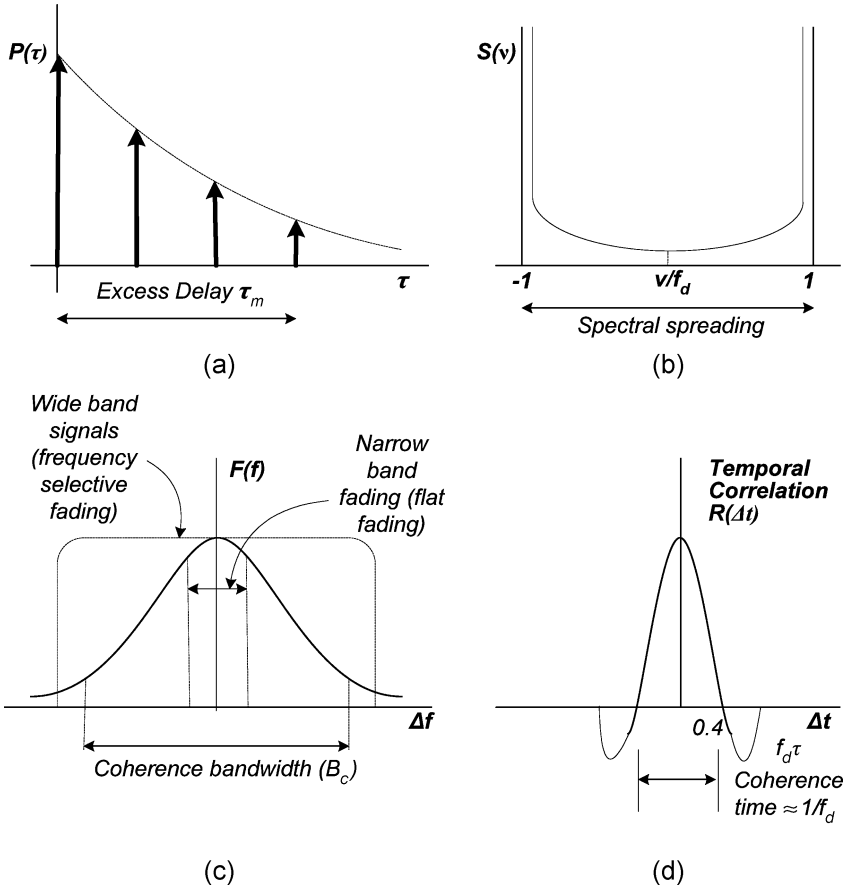


**Fig. 2.** ***Time and frequency dispersions in a mobile channel. (a) Power delay profile, (b) Doppler spectrum, (c) frequency correlation function, and (d) temporal correlation function.***

impulse response is determined by the values of the complex attenuations of the MPCs at time $t$. Equation (8) is valid for systems with large bandwidth,[1] so that we can resolve all the MPCs. Thus, there is no small-scale fading, and the only temporal change of the MPCs is a phase shift due to the change of runtime between the TX and RX as the mobile station (MS) (or the interacting objects) moves around.

In systems with reasonably small bandwidth (say, below 20 MHz), we can simplify the description further. Let us first introduce the concept of "resolvable delay bins." If an RX has a bandwidth $B$, then elementary Fourier analysis tells us that it can only distinguish signals that are approximately $\Delta = 1/B$ separated in the delay domain. We can thus divide the delay axis into bins of width $\Delta$. A discretized impulse response then reads[2]

$$h(t,m) = \sum \alpha_m(t)\delta(\tau - m\Delta). \qquad (9)$$

Note that now the coefficients $\alpha_m$ do consist of the superposition of MPCs, so that fading occurs for each of the resolvable delay bins. If the number of MPCs falling into a delay bin is large, then the fading statistics are complex Gaussian, as discussed in Section IV. Otherwise, different fading statistics, like Nakagami fading, might become suitable. If a line-of-sight exists between TX and RX, then the amplitude fading statistics in the first delay bin is usually Rice-distributed.

Often it is useful to describe the channel characteristics averaged over the small-scale fading. While the *mean* of the channel response is often zero (since the phases of the MPCs are uniformly distributed over the small-scale fading), the mean squared magnitude, also known as the power delay profile (PDP), is [see Fig. 2(a)][3]

$$P(\tau) = E_t\left\{|h(t,\tau)|^2\right\} \qquad (10)$$

[1]An exception will be discussed in Section IV-D.

[2]The above description is only approximate. A more accurate formulation relies on a sampled representation of the impulse response such that the sampling rate is at least equal to the Nyquist rate.

[3]Fig. 2 is a classic figure showing the time and frequency dispersion of a mobile channel and appears in many fundamental texts of wireless communications.

where $E_t$ denotes expectation over a time interval over which only small-scale fading happens.[4] This can be given an important physical interpretation: it is the received average power $P$ versus propagation delay $\tau$. The *root mean square (rms) delay spread* is the second central moment of the PDP [32]

$$\tau_{\mathrm{rms}} = \sqrt{\frac{\int_{-\infty}^{\infty} P(\tau)\tau^2 d\tau}{\int_{-\infty}^{\infty} P(\tau) d\tau} - \left(\frac{\int_{-\infty}^{\infty} P(\tau)\tau d\tau}{\int_{-\infty}^{\infty} P(\tau) d\tau}\right)^2}. \quad (11)$$

Many papers report the measured rms delay spread (and not complete PDPs) to characterize the delay dispersion; see also Section V-C.

### B. Frequency-Domain Interpretation

For many applications in CR, it is useful to transform the impulse response into the Fourier domain. As there are two temporal variables, there are also two transform pairs. Absolute time $t$ in (8) corresponds to Doppler frequency $\nu$, while delay $\tau$ corresponds to frequency $f$. In this section, we deal with the latter case; time variations and their Fourier transformation are treated in Section VI.

A Fourier transformation $\tau \Rightarrow f$ results in the time-variant *transfer function* $H(t, f)$. The Fourier transformation of the PDP also has an important meaning. To put it simply, the Fourier transform $F(f)$ of $P(\tau)$ [see Fig. 2(c)] is the frequency correlation function, i.e., a measure of how correlated the fading is from one frequency to another $f$ Hz away. If fading is highly correlated over a frequency interval of width $\Delta f$ (i.e., $F(f) \sim 1$ up to $\Delta f$) and a deep fade from a wireless TX to a CR RX is detected at some frequency $f_o$, then that fade can be assumed to occupy a band of width $\Delta f$ about $f_o$. Thus, an agile CR TX can send signals to that RX over that frequency interval without severe interference from the interfering TX. The coherence bandwidth $B_c$ is defined as the smallest frequency separation such that $|F(B_c)/F(0)| < k$, where $k$ has been given by different authors as 0.5, 0.75, and 0.9. The coherence bandwidth can be related to the delay spread as [33]

$$B_c \geq \frac{\arccos(k)}{2\pi} \frac{1}{\tau_{\mathrm{rms}}}. \quad (12)$$

A simpler, approximate estimation of $B_c$ is given in [34] for $k = 0.5$, namely, $B_c \approx 1/5\tau_{\mathrm{rms}}$.

Two cases must be distinguished to illustrate the role of coherence bandwidth [20] [see Fig. 2(c)]:

- a case where the signal bandwidth is less than $B_c$; this is commonly known as *flat fading* (transfer function is flat across the signal bandwidth);
- a case where the signal bandwidth is more than $B_c$; this is commonly known as *frequency-selective fading*.

The frequency correlation function and coherence bandwidth are also important for the sensing phase of CR, as the detection of radiation from other possible users is often done by "scanning" the spectrum. A single (narrowband) measurement of the arriving power in the frequency domain might not allow the detection of another user if its transfer function is in a fading dip. The frequency correlation function gives an indication of how densely a spectrum has to be sampled to avoid this problem.

### C. Models for the Delay Dispersion

The most common model for the power delay profile is the exponential model, i.e., $P(\tau) = \exp[-\gamma\tau]$ for $\tau \geq 0$, where $1/\gamma$ is the decay time constant [21]. It is noteworthy that for this model, the rms delay spread is identical to the decay time constant. We can also provide a tapped delay line model

$$A_i = c \exp\left(\frac{-i}{B\tau_{\mathrm{rms}}}\right), \quad i = 0, 1, 2, 3, \ldots \quad (13)$$

where $c$ is a normalizing constant, $B$ is the signal bandwidth, and $\tau_{\mathrm{rms}}$ is the rms delay spread, defined in (11). Several measurements have also found more complex power profiles that consist of several clusters.

It follows from the above derivations that the rms delay spread is obtained from impulse responses taken over an area in which small-scale fading occurs. In different such small-scale areas, $\tau_{\mathrm{rms}}$ can take on different values. It is useful to interpret those different values of $\tau_{\mathrm{rms}}$ as different realizations of a random variable and investigate its probability density function. Following [35], it is well approximated as

$$\tau_{\mathrm{rms}} = T_1 d^{\epsilon} y \quad (14)$$

where $d$ is in kilometers; $y$ is a lognormal variate whose dB value has zero mean and standard deviation $\sigma$; and $T_1$ is the median delay spread at $d = 1$ km. Numerical values for the parameters $T_1$, $\epsilon$, and $\sigma$ are tabulated in [35] for different environments. They show, for example, that $\varepsilon = 0.5$ in urban and suburban environments and $\varepsilon = 1$ in mountainous regions.

Many other measurements for rms delay spread can be found in the literature. Typical values for different environments are (see [36]) are as follows.

- *Indoor residential buildings:* Delay spreads of 5–10 ns are typical; but values up to 30 ns have been measured [37], [38]
- *Indoor office environments:* These typically show delay spreads between 10 and 100 ns, but even

[4]The above definition actually requires the assumption of ergodicity of the channel [11, App. 6A].

values of 300 ns have been measured. The room size has a clear influence on the delay spread; also building size and shape have an impact [39]–[47].

- *Factories and airport halls:* These have delay spreads that range from 50 to 200 ns [48], [49].
- *Microcells:* Delay spreads range from around 5–100 ns (for LOS situations) to 100–500 ns (for NLOS) [50]–[54].
- *Tunnels and mines:* Empty tunnels typically show a very small delay spread (on the order of 20 ns), while car-filled tunnels exhibit larger values (up to 100 ns) [55], [56].
- *Typical urban and suburban environments:* These show delay spreads between 100 and 800 ns, although values up to 3 $\mu$s have also been observed [54], [57]–[61].
- *Bad urban and hilly terrain environments:* These show clear examples of multiple clusters that lead to much larger delay spreads. Delay spreads up to 18 $\mu$s, with cluster delays of up to 50 $\mu$s, have been measured in various European cities, while American cities show somewhat smaller values. Cluster delays of up to 100 $\mu$s occur in mountainous terrain [60], [62]–[69].

### D. Ultra-Wide-Band Channels

UWB channels are usually defined as channels with either large relative ($> 20\%$) or large absolute ($> 500$ MHz) bandwidth. For the case of large relative bandwidth, the impulse response consists of a sum of delayed, *distorted* pulses, i.e.,

$$h(\tau) = \sum_{i=1}^{N} a_i \chi_i(\tau) \otimes \delta\left(\tau - \tau_{i(t)}\right) \tag{15}$$

where $\chi_i(\tau)$ denotes the distortion of the $i$th MPC. The distortion is created by the frequency selectivity of the interaction process (e.g., because the reflection coefficient depends on frequency when a large relative frequency range is considered). In addition to those delay characteristics, we also find that the directional characteristics and shadowing can depend on the absolute frequency. It is also noteworthy that the delay of the MPCs can change with time; specifically, the changes can occur on the same time scale as Rayleigh fading. When considering the transfer function, the pulse distortion corresponds to a different *average* attenuation at different frequencies (usually higher frequencies are more strongly attenuated than lower frequencies); this fact should be taken into account when planning UWB CR systems.

Systems with large absolute bandwidth have very fine delay resolution, so that each resolvable delay bin may contain only very few MPCs. As a consequence, Gaussian fading statistics might not hold for each bin. There are still many unknown aspects of UWB channels; an overview of the current state of research is given in [71] and [72].

## VI. FREQUENCY DISPERSION

In Section IV, we discussed time variations of the channel and their importance for CR. In this section, we use an alternative mathematical description, namely, that time variations also lead to a frequency dispersion. This fact can be interpreted simply as a consequence of Fourier theory. We can thus obtain a different representation of the time-variant impulse response by Fourier transformation $t \Rightarrow \nu$. This gives the *delay-Doppler spread function* $s(\nu, \tau)$, also known simply as *spreading function*. A physical interpretation is the following: the movement of the MS or scatterers leads to frequency shifts of an MPC, due to the Doppler effect. Note that the Doppler shift depends on the angle between the MPC and the direction that a scatterer is moving. Since different MPCs have different angles, this gives rise to a *spreading* of the signal in the frequency domain: a transmitted sinusoidal wave leads to a receive signal with a spectrum that extends over a whole range of frequencies. It is important to note that in the case of mobile TX or RX, *all* MPCs undergo temporal changes and thus phase shifts, while in the fixed-wireless case, only *some* MPCs (the ones associated with moving scatterers) change; the latter case suggests the notion of a temporal Ricean $K$-factor, as described in Section IV.

By averaging over the small-scale fading (including averaging over all delays), we can obtain the *Doppler spectrum*

$$S(\nu) = E_\tau\left\{|s(\nu, \tau)|^2\right\} \tag{16}$$

whose Fourier transformation $R(\Delta t)$ is the temporal coherence function.

The most commonly used Doppler spectrum in mobile environments is the Jakes spectrum [21] [see Fig. 2(b)]. For a particular case of scatterers that are uniformly distributed $[0,2\pi]$, [21] has established a closed-form relationship for $S(\nu)$

$$S(\nu) = \begin{cases} \frac{P_r}{2\pi f_d} \frac{1}{\sqrt{1-\left(\frac{|\nu - f_c|}{f_d}\right)^2}}, & |\nu - f_c| \le f_d \\ 0, & \text{elsewhere} \end{cases} \tag{17}$$

where $P_r$ is the total received power, $f_d$ is the maximum Doppler frequency given by $v/\lambda$, and $f_c$ is the carrier frequency. This corresponds to a temporal correlation that is equal to $J_0(2\pi f_d \tau)$; see Fig. 2(d) [11], [22].

In the fixed-wireless case, the Doppler spectrum of the time-varying MPCs is better approximated by zero-mean complex Gaussian process whose power density spectrum

about the center frequency is proportional to the truncated function [19]

$$S(\nu) = \begin{cases} 1 - 1.72\left(\frac{\nu}{f_m}\right)^2 + 0.785\left(\frac{\nu}{f_m}\right)^4, & |\nu| < f_m \\ 0, & \text{otherwise} \end{cases} \quad (18)$$

where the truncation frequency $f_m$ scales linearly with the center frequency and is about 3.6 Hz at a center frequency of 2.5 GHz [73].

## VII. ANGLE DISPERSION

### A. Modeling

The MPCs are characterized not only by their delay but also by their directions. An MPC leaves the TX in a certain direction (determined by the location of the first scatterer it will encounter) and arrives at the RX in a certain direction (similarly determined by the position of the last scatterer before arrival). Since there are many MPCs, which can depart and arrive in different directions, a multipath channel leads to angular dispersion. This angular dispersion is very important for CR: it determines the ability of adaptive antennas to transmit into such directions that they will not disturb other users located in certain directions. A small angular spread offers the possibility of precisely focusing beams into particular directions.

A description of the angular dispersion can be made by generalizing the concept of impulse response. The double-directional impulse response (DDIR), which generalizes (8), again consists of a sum of contributions from the MPCs [74]

$$h(t, \tau, \Omega, \Psi) = \sum_{l=1}^{L(t)} a_l \delta(\tau - \tau_l)\delta(\Omega - \Omega_l)\delta(\Psi - \Psi_l) \quad (19)$$

where the $\Omega_l$ are the directions-of-departure and the $\Psi_l$ are the directions-of-arrival, and $L(t)$ is the number of MPCs. From the double-directional impulse response, we can also easily derive the joint impulse response or transfer function of the different elements in an antenna array, also known as the "channel transfer function matrix" [11, Sec. 6.7].

The DDIR is a quite general description of the channel.[5] From it, we can derive the "normal" time-variant impulse response by weighting the DDIR with the antenna pattern and then integrating over all angles

$$h(t, \tau) = \int\int h(t, \tau, \Omega, \Psi)\widetilde{G}_t(\Omega)\widetilde{G}_r(\Psi)d\Omega d\Psi \quad (20)$$

[5]An even more general description includes the polarization of the MPCs; see [75], [76].

where $\widetilde{G}_t$ and $\widetilde{G}_r$ are the complex amplitude antenna patterns (in linear units) for the TX and RX antenna, respectively; note that $G_t = 20\log|\widetilde{G}_t|$ and similarly for $G_r$.

The angular power spectrum (APS) is a characterization of how much power arrives on average from a certain angle. For example, when considering the APS at the TX

$$\text{APS}(\Omega) = E\{|h(t, \tau, \Omega, \Psi)|^2\}. \quad (21)$$

As will be further discussed in Section VIII, this APS can be a function of $\tau$ and $\Psi$, or averaged over those variables.

A compact characterization of the angular dispersion is often done by the angle spread or rms angle spread (AS) [77]. As mentioned above, angular dispersion causes space-selective fading, which means that signal amplitude depends upon the space location of the antenna. The spatial coherence distance is inversely related to the rms AS. Antenna elements must be located at distances larger than the coherence distance so that they experience independent fading. It must also be emphasized that in an environment with static scatterers and moving TX or RX, the angular dispersion is strongly related to the Doppler effect because the directions of the MPCs determine their Doppler shifts; however, this is *not* true in the fixed wireless case.

### B. Typical Values of Angular Dispersion

The most common model for the APS at an *elevated* TX or RX is a small angular spread around the nominal line-of-sight direction, usually with a Laplacian APS [78]

$$\text{APS}(\phi) = \exp\left[-\sqrt{2}\frac{|\phi - \phi_0|}{S_\phi}\right] \quad (22)$$

where $\phi_0$ is the mean azimuthal angle and $S_\phi$ is the AS. The elevation spectrum is usually modeled as a delta function (i.e., all radiation is incident in the horizontal plane) so that $\Omega = \phi$. The most common model for the APS at a TX or RX at street level is a distribution that is uniform in azimuth.

Similar to the case of the delay spread, many papers give only the rms angular spread as the result of measurement campaigns, though some give the cluster rms spread. While fewer papers deal with angular dispersion than with delay dispersion, the following range of values can be considered typical.

- *Indoor office environments:* Cluster angular spreads between 10° and 20° have been observed for NLOS situations; for LOS situations, they are considerably smaller [46], [79].
- *Industrial environments:* Angular spreads between 20° and 30° have been observed [48].

- *Microcells:* Angular spreads between 5° and 20° for LOS and 5° and 40° for NLOS have been found in [69], [80], and [81].
- *Typical urban and suburban environments:* In urban environments, [82] and [83] measured angular spreads on the order of 3°–20° degrees, while [84] found angular spreads of up to 40°. In suburban environments, the angular spread was usually smaller than 5° due to a frequent occurrence of LOS [82].
- *Bad urban and hilly terrain environments:* These show around 20° and up total angular spread due to the existence of multiple clusters [69], [85].
- *Rural environments:* Angular spreads between 1° and 5° have been observed [81].

For a *street-level* TX or RX, various investigations have been made into the actual shape of the APS. The "standard" model, i.e., an APS that is uniform in azimuth, stems from Jakes [21] and was used until the 1990s. However, recent studies indicate that the azimuthal spread can be considerably smaller, especially in street canyons. The azimuthal power spectrum often is approximated as Laplacian as in (22); another proposal is the von Mises pdf [86].

## VIII. JOINT DISPERSION CHARACTERISTICS AND POLARIZATION

In the previous sections, we have treated delay dispersion, frequency dispersion, and angular dispersion as separate effects. However, there are some important interrelations among them. First, the rms delay spread, rms angle spread, and shadowing are correlated. Furthermore, the shape of the frequency dispersion is a function of delay, etc. Here, we briefly discuss these topics, which the interested reader can pursue using the references we cite. We also briefly discuss radio signal polarization and its possible relevance to CR systems.

### A. Three Types of Spread

From the above discussion, the time/frequency selectivity of a wireless channel can be defined by three spreads [87], [88]: delay spread, angle spread, and Doppler spread. In outdoor environments, the distribution of the angular spread over large areas has been found to be lognormal and correlated with the delay spread (correlation coefficient approximately 0.5) [89]. Actually, delay spread, angular spread, and shadowing are a triplet of correlated lognormal variables, with correlation of angular spread to shadowing being around 0.75 [29], and similarly for the correlation between delay spread and shadowing [35]. Also for indoor peer-to-peer environments, a correlation between delay spread and angular spread has been observed [90].

These correlations have an impact on the planning of CRs. For example, the correlation between shadowing and delay spread helps in wide-band sensing: in the shadowing fades, where detection of a primary radio is basically more difficult, the increased delay dispersion helps to average out the small-scale fading and thus decrease the fading margin (which is normally needed to decrease the missed-detection probability).

We also note that the three types of spread are not a complete description of the dispersion characteristics. A full description of the joint second-order statistics of the dispersion is given by the double-directional delay power spectrum (DDDPS) [77], [91]. While many papers in the literature assume that the DDDPS can be decomposed into a product of PDP, APS at the TX, and APS at the RX, several experimental investigations indicate that such a factorization is an oversimplification—e.g., the APS *does* depend on the delay [92]–[95]. This is especially true in the case where the multipath components are arriving in clusters [76], [96]–[98].

### B. Polarization

When multiple antennas are required at the TX or RX, the antennas used could be an array of copolarized elements, typically using vertical ($V$) polarization. However, there is increased interest in using polarized diversity, i.e., antennas that are colocated but receive both polarizations. In this case, the gains of diversity rely on the polarization mixing of the transmitted signals, which happens as a consequence of the wireless channel.

Polarization is important for calculating the interference from CR to polarized directional microwave transmission. Polarization discrimination can also play a useful role in CR, as systems might be able to use polarization components that other devices are not strongly exciting. As a first approximation, parameters like delay spread, angular spread, etc., are the same for vertical and horizontal polarizations for NLOS situations. The fading of the components is independent; and the *average* power leakage between the two polarizations is given by the cross-polarization discrimination (XPD). This is defined as the ratio $P_{VV}/P_{VH}$, where $P_{VV}$ is the power of a $V$ polarized transmitted signal received as $V$ polarized; and $P_{VH}$ is the power of a $V$ polarized transmitted signal received as H polarized. The XPD is distance dependent but is also influenced by the multipath environment [75].

Values for the XPD in LOS indoor situations are above 10 dB, in indoor NLOS situations around 3 dB [101], in urban outdoor 5 dB, and in suburban outdoor environments 12 dB [102]. More generally, the XPD is a function of the excess path loss: high path loss (which also implies no LOS) generally leads to low XPD [103].

## IX. SUMMARY OF KEY PARAMETERS OF THE WIRELESS CHANNEL MODELS

We have reviewed the models that are used to define the propagation conditions of the wireless systems operating in different locales. The list of references containing measurements is very extensive. Here we give a summary of selected references where key parameters of these

models may be found and that have been standardized by national or international organizations, and/or are often used by industry practitioners and system designers.

### A. Path Loss Models

The best known path-loss model and its empirical parameters for the cellular environment with base-station height above rooftops (macrocells) is given by Hata in [2] and is based on measurements in Japan [12]. These measurements were made in frequency bands below 1 GHz. An extension to the 1.8 GHz band is given in [13]; this reference also gives a model (based on both theory and measurements) for cellular environments where the base-station height is comparable to, or lower than, rooftop height (microcells). Standardized values for the 2 GHz band are given in [104]. The broadcasting bands use very high towers (often located on prominent hilltops) and use large (kilowatt) transmit powers. The field strength of these systems is calculated using the models given in [105]. Path-loss models for fixed wireless access systems are given in [17] and [19].

### B. Ricean K-Factor Models

Extensive measurements of the $K$-factor and empirical relationships are given in [25]. These measurements were made in European cities in the 5 GHz band. Temporal $K$-factor measurements in the 2 GHz band and used in fixed wireless access systems are given in [19].

### C. Delay Dispersion Models

A considerable number of standardized multipath delay profiles exist. We first discuss models for macrocellular environments. Reference [106] gives profiles based on measurements in Europe for a 900 MHz carrier frequency and a 200 kHz bandwidth. A model for higher bandwidth (5 MHz) and carrier frequency (2 GHz) was standardized by the ITU in [104]; this model is mainly intended for macrocellular environments. More refined models for macro- and microcells can be found in [29], [97], and [107], as discussed below.

For indoor environments, [109] and [110] give power delay profiles suitable for systems with a 20 MHz bandwidth; the models are used for both the 2 GHz and the 5 GHz bands. Ultra-wide-band channel models, which cover the whole band between 3 and 10 GHz, can be found in [111]–[113].

### D. Frequency Dispersion Models

Most people use the classic Jakes spectrum [21]. Indeed, this is the case for the ITU standard [104]. Similarly, [106] defines Doppler spectra that are either Jakes-like or Gaussian in shape for the different taps of the power delay profile in macrocellular environments. Doppler spectra peaked at the center tend to occur more frequently in fixed-wireless applications, while Doppler spectra with a "bathtub" shape correspond more to a mobile station moving on a street.

### E. Comprehensive Models

Recently, several models have been developed that describe path loss, delay dispersion, and angular dispersion (and thus implicitly Doppler spectra). For both macrocellular and microcellular environments, [107] gives models for a 5 MHz bandwidth and a 2 GHz carrier frequency. An indoor model that includes delay dispersion and angular dispersion is described in [114]. More refined models that are suitable for even more environments can be found in [29], [76], [97], [95], and [108].

### F. Usage of Models

The models we presented above—and, more generally, any statistical channel model—cannot completely describe the reality of propagation. "Typical" or "standardized" values of channel parameters are helpful in comparing different radio systems to each other, but they can deviate from the physical reality. Therefore, no performance guarantees can be given for CR based on channel models, nor can a "noninterference" guarantee be provided.

## X. CONCLUSION

Wireless channel models like those described here are critical to both the analysis of interference to primary receivers in CR environments and the design of real-time methods to control such interference. Some examples are as follows.

- Models of path loss and its distance dependence help to predict the median interference powers at primary receivers.
- Models of shadow fading and its spatial variability help to relate power measurements on CR–CR paths to interference levels over CR–primary paths.
- Models of fading statistics (e.g., the Ricean K-factor) help 1) to determine the needed fade margins on CR–CR paths and 2) to predict the statistical variability of CR–primary interference.
- Models of rms delay spread and/or frequency correlation bandwidth help to relate power measurements at one frequency to interference levels at another.
- Models of angular spread help to predict the ability of a CR system to suppress interference in the direction of the primary receiver.
- All these models make it possible for system analysts and designers to simulate propagation environments and then evaluate candidate CR algorithms for interference mitigation, leading to optimized designs and more reliable performance predictions.

This paper has reviewed the current state of the art in wireless channel models. There are two key aspects of this topic: models for path loss and models for channel impulse response. We have provided a summary of models for both aspects and references for the model parameters. Most of all, we have attempted to relate the

various properties of wireless channel models to their potential use in the design of CRs. This is certainly a topic that bears further thought and research. ■

## Acknowledgment

The authors would like to thank Prof. Simon Haykin and the anonymous reviewers for valuable suggestions that improved the clarity of the paper. The authors gratefully acknowledge the help of M. F. Hanif, Ph.D. student at the Department of Electrical and Computer Engineering, University of Canterbury, U.K., for typesetting the document and making the diagrams, and Mr. Michael Williams, Technical Writer, Telecom New Zealand, in proof reading the various manuscripts of this article.

## REFERENCES

[1] S. Haykin, "Cognitive radio: Brain-empowered wireless communications," *IEEE J. Sel. Areas Commun.*, vol. 23, pp. 201–220, Feb. 2005.

[2] M. Hata, "Empirical formula for propagation loss in land mobile radio services," *IEEE Trans. Veh. Technol.*, vol. VT-29, pp. 317–325, Aug. 1980.

[3] E. Hossain and V. K. Barghava, Eds., *Cognitive Wireless Communication Networks*. New York: Springer, 2008.

[4] I. F. Akyildiz, W. Y. Lee, M. C. Vuran, and S. Mohanty, "Next generation/dynamic spectrum access/cognitive radio wireless networks: A survey," *Comput. Netw.*, vol. 50, no. 13, pp. 2127–2159, 2006.

[5] D. A. Roberson *et al.*, "Spectral occupancy and interference studies in support of cognitive radio technology deployment," in *Proc. 1st IEEE Workshop Net Technol. SDR Netw.*, 2006.

[6] Q. Zhao and B. M. Sadler, "A survey of dynamic spectrum access," *IEEE Signal Process. Mag.*, vol. 24, no. 3, pp. 79–89, 2007.

[7] S. Srinivasa and S. Jafar, "The throughput potential of cognitive radio: A theoretical perspective," *IEEE Commun. Mag.*, vol. 45, no. 5, pp. 73–79, 2007.

[8] Z. Quan, S. Ciu, A. H. Sayed, and H. V. Poor, "Wideband spectrum sensing in cognitive radio networks," in *Proc. IEEE Int. Conf. Commun.*, 2008.

[9] J. Zhu and K. J. R. Liu, "Cognitive radios for dynamic spectrum access—Dynamic spectrum sharing: A game theoretical overview," *IEEE Commun. Mag.*, vol. 45, no. 5, pp. 88–94, 2007.

[10] N. Devroye, P. Mitran, and V. Tarokh, "Achievable rates in cognitive radio channels," *IEEE Trans. Inf. Theory*, vol. 52, no. 5, pp. 1813–1827, 2006.

[11] A. F. Molisch, *Wireless Communications*. New York: IEEE-Wiley, 2005.

[12] Y. Okumura, E. Ohmori, T. Kawano, and K. Fukuda, "Field strength and its variability in UHF and VHF land-mobile radio service," *Rev. Electr. Commun. Lab.*, vol. 16, no. 9, 1968.

[13] European Co-operative in the Field of Science and Technical Research, "Urban transmission loss models for mobile radio in the 900 and 1800 MHz bands," Tech. Rep., EURO-COST 231, Rev. 2, Sep. 1991.

[14] V. Erceg, L. J. Greenstein, S. Y. Tjandra, S. R. Parkoff, A. Gupta, B. Kulic, A. A. Julius, and R. Bianchi, "An empirically based path loss model for wireless channels in suburban environments," *IEEE J. Sel. Areas Commun.*, vol. 17, pp. 1205–1211, Jul. 1999.

[15] T. S. Chu and L. J. Greenstein, "A quantification of link budget differences between the cellular and PCS bands," *IEEE Trans. Veh. Technol.*, vol. 48, pp. 60–65, Jan. 1999.

[16] W. C. Jakes, Jr. and D. O. Reudink, "Comparison of mobile radio transmission at UHF and X band," *IEEE Trans. Veh. Technol.*, vol. VT-16, pp. 10–14, Oct. 1967.

[17] K. V. S. Hari *et al.*, "Interim channel models for G2 MMDS fixed wireless applications," IEEE 802.16.3c-00/49r2.

[18] M. S. Smith and C. Tappenden, "Additional enhancements to interim channel models for G2 MMDS fixed wireless applications," IEEE 802.16.3c-00/53.

[19] V. Erceg, "Channel models for fixed wireless applications," IEEE 802.16d-03/34.

[20] A. F. Molisch, *Wideband Wireless Digital Communications*. New York: Prentice-Hall, 2000.

[21] W. C. Jakes, *Microwave Mobile Communications*. New York: Wiley, 1974.

[22] A. Goldsmith, *Wireless Communications*. New York: Cambridge Univ. Press.

[23] T. S. Rappaport, *Wireless Communications: Principles and Practice*, 2nd ed. Englewood Cliffs, NJ: Prentice-Hall, 2001.

[24] H. L. Bertoni, W. Honcharenko, L. R. Macel, and H. H. Xia, "UHF propagation prediction for wireless personal communications," *Proc. IEEE*, vol. 82, pp. 1333–1359, Sep. 1994.

[25] "Final report on link level and system level channel models," Tech. Rep. IST-2003-507581.

[26] M. Gudmundson, "Correlation model for shadow fading in mobile radio systems," *Electron. Lett.*, vol. 27, no. 23, pp. 2145–2146, Nov. 7, 1991.

[27] J. Weitzen and T. J. Lowe, "Measurement of angular and distance correlation properties of log-normal shadowing at 1900 MHz and its application to design of PCS systems," *IEEE Trans. Veh. Technol.*, vol. 51, pp. 265–273, Mar. 2002.

[28] L. J. Greenstein and V. Erceg, "Gain reductions due to scatter on wireless paths with directional antennas," *IEEE Commun. Lett.*, vol. 3, pp. 169–171, Jun. 1999.

[29] H. Asplund, A. A. Glazunov, A. F. Molisch, K. I. Pedersen, and M. Steinbauer, "The COST259 directional channel model part II: Macrocells," *IEEE Trans. Wireless Commun.*, vol. 5, pp. 3434–3450, Dec. 2006.

[30] L. J. Greenstein *et al.*, "Ricean K-factors in narrowband fixed wireless channels: Theory, experiments and statistical models," *IEEE Trans. Veh. Technol.*, to be published.

[31] D. S. Baum *et al.*, "Measurements and characterization of broadband MIMO fixed wireless channels at 2.5 GHz," in *Proc. ICPWC*, Dec. 2000.

[32] A. F. Molisch and M. Steinbauer, "Condensed parameters for characterizing wideband mobile radio channels," *Int. J. Wireless Inf. Netw.*, 1999.

[33] B. H. Fleury, "An uncertainty relation for WSS processes and its application to WSSUS systems," *IEEE Trans. Commun.*, vol. 44, pp. 1632–1634, 1996.

[34] B. Sklar, "Rayleigh fading channels in mobile digital communication systems: I. Characterization," *IEEE Commun. Mag.*, vol. 35, pp. 136–146, Sep. 1997.

[35] L. J. Greenstein, V. Erceg, Y. S. Yeh, and M. V. Clark, "A new path-gain/delay-spread propagation model for digital cellular channels," *IEEE Trans. Veh. Technol.*, vol. 46, pp. 477–485, May 1997.

[36] A. F. Molisch and F. Tufvesson, "Multipath propagation models for broadband wireless systems," in *Handbook of Signal Processing for Wireless Commmunications*, ch. 2, M. Ibnkahla, Ed. Boca Raton, FL: CRC Press, 2004.

[37] S. S. Ghassemzadeh, R. Jana, C. W. Rice, W. Turin, and V. Tarokh, "Measurement and modeling of an ultra-wide bandwidth indoor channel," *IEEE Trans. Commun.*, vol. 52, pp. 1786–1796, Oct. 2004.

[38] J. MacLellan, S. Lam, and X. Lee, "Residential indoor RF channel characterization," in *Proc. IEEE Veh. Technol. Conf.*, 1993, pp. 210–213.

[39] C. Bergljung and P. Karlsson, "Propagation characteristics for indoor broadband radio access networks in the 5 GHz band," in *Proc. IEEE Int. Symp. Pers., Indoor Mobile Radio Commun.*, 1998, pp. 612–616.

[40] I. Cuinas and M. G. Sanchez, "Measuring, modeling, and characterizing of indoor radio channel at 5.8 GHz," *IEEE Trans. Veh. Technol.*, vol. 50, pp. 526–535, Mar. 2001.

[41] D. Devasirvatham, "Time delay spread and signal level measurements of 850 MHz radio waves in building environments," *IEEE Trans. Antennas Propagat.*, vol. AP-34, pp. 1300–1305, Nov. 1986.

[42] D. Devasirvatham, "A comparison of time delay spread and signal level measurements within two dissimilar office buildings," *IEEE Trans. Antennas Propagat.*, vol. AP-35, pp. 319–324, Mar. 1987.

[43] H. Hashemi and D. Tholl, "Statistical modeling and simulation of the RMS delay spread of indoor radio propagation channels," *IEEE Trans. Veh. Technol.*, vol. 43, pp. 110–120, Feb. 1994.

[44] P. Karlsson, C. Bergljung, E. Thomsen, and H. Borjeson, "Wideband measurement and analysis of penetration loss in the 5 GHz band," in *Proc. IEEE Veh. Technol. Conf.*, 1999, pp. 2323–2328.

[45] J. Medbo, H. Hallenberg, and J. E. Berg, "Propagation characteristics at 5 GHz in typical radio-LAN scenarios," in *Proc. IEEE Veh. Technol. Conf.*, 1999, pp. 185–189.

[46] Q. H. Spencer, B. D. Jeffs, M. A. Jensen, and A. L. Swindlehurst, "Modeling the statistical time and angle of arrival characteristics of an indoor multipath channel," *IEEE J. Sel. Areas Commun.*, vol. 18, pp. 347–360, Mar. 2000.

[47] L. Talbi and G. Y. Delisle, "Experimental characterization of EHF multipath indoor

radio channels," *IEEE J. Sel. Areas Commun.*, vol. 14, pp. 431–440, Apr. 1996.

[48] D. Hampicke, A. Richter, A. Schneider, G. Sommerkorn, R. S. Thoma, and U. Trautwein, "Characterization of the directional mobile radio channel in industrial scenarios, based on wideband propagation measurements," in *Proc. Veh. Technol. Conf.*, 1999, pp. 2258–2262.

[49] T. S. Rappaport, "Characterization of UHF multipath radio channels in factory buildings," *IEEE Trans. Antennas Propagat.*, vol. 37, pp. 1058–1069, Aug. 1989.

[50] A. A. Arowojolu, A. M. D. Turkmani, and J. D. Parsons, "Time dispersion measurements in urban microcellular environments," in *Proc. IEEE Veh. Technol. Conf.*, 1994, pp. 150–154.

[51] M. J. Feuerstein, K. L. Blackard, T. S. Rappaport, S. Y. Seidel, and H. H. Xia, "Path loss, delay spread, and outage models as functions of antenna height for microcellular system design," *IEEE Trans. Veh. Technol.*, vol. 43, pp. 487–498, Aug. 1994.

[52] S. Kozono and A. Taguchi, "Mobile propagation loss and delay spread characteristics with a low base station antenna on an urban road," *IEEE Trans. Veh. Technol.*, vol. 42, pp. 103–109, Feb. 1993.

[53] J. Wiart, P. Pajusco, A. Levy, and J. C. Bic, "Analysis of microcellular wide band measurements in paris," in *Proc. IEEE Int. Symp. Pers., Indoor Mobile Radio Commun.*, 1995, pp. 144–147.

[54] X. Zhao, J. Kivinen, P. Vainikainen, and K. Skog, "Propagation characteristics for wideband outdoor mobile communications at 5.3 GHz," *IEEE J. Sel. Areas Commun.*, vol. 20, pp. 507–514, Apr. 2002.

[55] M. Lienard and P. Degauque, "Natural wave propagation in mine environments," *IEEE Trans. Antennas Propagat.*, vol. 48, pp. 1326–1339, Sep. 2000.

[56] Y. P. Zhang and Y. Hwang, "Characterization of uhf radio propagation channels in tunnel environments for microcellular and personal communications," *IEEE Trans. Veh. Technol.*, vol. 47, pp. 283–296, Feb. 1998.

[57] A. Kanatas, N. Moraitis, G. Pantos, and P. Constantinou, "Wideband characterization of microcellular suburban mobile radio channels at 1.89 GHz," in *Proc. IEEE Veh. Technol. Conf.*, 2002, pp. 1060–1064.

[58] J. F. Kepler, T. P. Krauss, and S. Mukthavaram, "Delay spread measurements on a wideband mimo channel at 3.7 GHz," in *Proc. IEEE Veh. Technol. Conf.*, 2002, pp. 2498–2502.

[59] I. Oppermann, J. Talvitie, and D. Hunter, "Wide-band wireless local loop channel for urban and sub-urban environments at 2 GHz," in *Proc. IEEE Int. Conf. Commun.*, 1997, pp. 61–65.

[60] T. S. Rappaport, S. Y. Seidel, and R. Singh, "900-MHz multipath propagation measurements for US digital cellular radiotelephone," *IEEE Trans. Veh. Technol.*, vol. 39, pp. 132–139, May 1990.

[61] E. S. Sousa, V. M. Jovanovic, and C. Daigneault, "Delay spread measurements for the digital cellular channel in Toronto," *IEEE Trans. Veh. Technol.*, vol. 43, pp. 837–847, Nov. 1994.

[62] J. E. Berg, J. Ruprecht, J. P. de Weck, and A. Mattsson, "Specular reflections from high-rise buildings in 900 MHz cellular systems," in *Proc. IEEE Veh. Technol. Conf.*, 1991, pp. 594–599.

[63] P. E. Driessen, "Prediction of multipath delay profiles in mountainous terrain," *IEEE J. Sel. Areas Commun.*, vol. 18, pp. 336–346, Mar. 2000.

[64] A. A. Glazunov, H. Asplund, and J. E. Berg, "Statistical analysis of measured short-term impulse response functions of 1.88 GHz radio channels in stockholm with corresponding channel model," in *Proc. IEEE Veh. Technol. Conf.*, 1999, pp. 107–111.

[65] A. Kuchar, J. P. Rossi, and E. Bonek, "Directional macro-cell channel characterization from urban measurements," *IEEE Trans. Antennas Propagat.*, vol. 48, pp. 137–146, Feb. 2000.

[66] U. Martin, "Spatio-temporal radio channel characteristics in urban macrocells," *Proc. Inst. Elect. Eng. Radar, Sonar Navig.*, vol. 145, pp. 42–49, Feb. 1998.

[67] W. Mohr, "Wideband propagation measurements of mobile radio channels in mountainous areas in the 1800 MHz frequency range," in *Proc. IEEE Veh. Technol. Conf.*, 1993, pp. 49–52.

[68] S. Y. Seidel, T. S. Rappaport, S. Jain, M. L. Lord, and R. Singh, "Path loss, scattering and multipath delay statistics in four European cities for digital cellular and microcellular radiotelephone," *IEEE Trans. Veh. Technol.*, vol. 40, pp. 721–730, Nov. 1991.

[69] M. Toeltsch, J. Laurila, K. Kalliola, A. F. Molisch, P. Vainikainen, and E. Bonek, "Statistical characterization of urban spatial radio channels," *IEEE J. Sel. Areas Commun.*, vol. 20, pp. 539–549, Apr. 2002.

[70] P. Bello, "Characterization of randomly time-variant linear channels," *IEEE Trans. Commun.*, vol. COM-11, pp. 360–393, Dec. 1963.

[71] A. F. Molisch, "Ultrawideband propagation channels-theory, measurement, and modeling," *IEEE Trans. Veh. Technol.*, vol. 54, pp. 1528–1545, Sep. 2005.

[72] A. F. Molisch, "Ultrawideband propagation channels and their impact on system design," in *Proc. IEEE Int. Symp. Microwave, Antenna, Propagat. EMC Technol. Wireless Commun.*, 2007, pp. 1–5.

[73] D. S. Baum, D. Gore, R. Nabar, S. Panchanathan, K. V. S. Hari, V. Erceg, and A. J. Paulraj, "Measurement and characterization of broadband MIMO fixed wireless channels at 2.5 GHz," in *Proc. IEEE Int. Conf. Pers. Wireless Commun.*, 2000, pp. 203–206.

[74] M. Steinbauer, A. F. Molisch, and E. Bonek, "The double-directional radio channel," *IEEE Antennas Propagat. Mag.*, vol. 43, pp. 51–63, Aug. 2001.

[75] M. Shafi, M. Zhang, A. L. Moustakas, P. J. Smith, A. F. Molisch, F. Tufvesson, and S. H. Simon, "Polarized MIMO channels in 3-D: Models, measurements and mutual information," *IEEE J. Sel. Areas Commun.*, vol. 24, pp. 514–527, Mar. 2006.

[76] A. F. Molisch, H. Asplund, R. Heddergott, M. Steinbauer, and T. Zwick, "The COST259 directional channel model, Part I: Overview and methodology," *IEEE Trans. Wireless Commun.*, vol. 5, pp. 3421–3433, Dec. 2006.

[77] B. H. Fleury, "First- and second-order characterization of direction dispersion and space selectivity in the radio channel," *IEEE Trans. Inf. Theory*, vol. 46, pp. 2027–2044, Sep. 2000.

[78] K. I. Pedersen, P. E. Mogensen, B. H. Fleury, F. Frederiksen, K. Olesen, and S. L. Larsen, "Analysis of time, azimuth, and doppler dispersion in outdoor radio channels," in Proc. ACTS Mobile Commun. Summit, Aalborg, Denmark, 1997, pp. 308–313.

[79] C.-C. Chong, C.-M. Tan, D. I. Laurenson, S. McLaughlin, M. A. Beach, and A. R. Nix, "A new statistical wideband spatio-temporal channel model for 5-GHz band WLAN systems," *IEEE J. Sel. Areas Commun.*, vol. 21, pp. 139–150, Feb. 2003.

[80] M. Chen and H. Asplund, "Measurements and models for direction of arrival of radio waves in LOS in urban microcells," in *Proc. IEEE Int. Symp. Pers., Indoor Mobile Radio Commun.*, 2001, pp. 100–104.

[81] P. Pajusco, "Experimental characterization of DOA at the base station in rural and urban area," in *Proc. IEEE Veh. Technol. Conf.*, 1998, pp. 993–997.

[82] M. Larsson, "Spatio-temporal channel measurements at 1800 MHz for adaptive antennas," in *Proc. IEEE Veh. Technol. Conf.*, 1999, pp. 376–380.

[83] K. I. Pedersen, P. E. Mogensen, and B. H. Fleury, "Power azimuth spectrum in outdoor environments," *Electron. Lett.*, vol. 33, pp. 1583–1584, Aug. 1997.

[84] P. Laspougeas, P. Pajusco, and J. C. Bic, "Radio propagation in urban small cells environment at 2 GHz: Experimental spatio-temporal characterization and spatial wideband channel model," in *Proc. IEEE Veh. Technol. Conf.*, 2000, pp. 885–892.

[85] J. Laurila, K. Kalliola, M. Toeltsch, K. Hugl, P. Vainikainen, and E. Bonek, "Wideband 3D characterization of mobile radio channels in urban environment," *IEEE Trans. Antennas Propagat.*, vol. 50, pp. 233–243, Feb. 2002.

[86] A. Abdi and M. Kaveh, "A space-time correlation model for multielement antenna systems in mobile fading channels," *IEEE J. Sel. Areas Commun.*, vol. 20, pp. 550–560, Apr. 2002.

[87] A. J. Paulraj and C. B. Papadias, "Space-time processing for wireless communications," *IEEE Signal Process. Mag.*, vol. 14, no. 6, pp. 49–83, Nov. 1997.

[88] A. J. Paulraj and B. C. Ng, "Space-time modems for wireless personal communications," *IEEE Pers. Commun.*, vol. 5, pp. 36–48, Feb. 1998.

[89] A. Algans, K. I. Pedersen, and P. E. Mogensen, "Experimental analysis of the joint statistical properties of azimuth spread, delay spread, and shadow fading," *IEEE J. Sel. Areas Commun.*, vol. 20, pp. 523–531, Apr. 2002.

[90] G. D. Durgin, V. Kukshya, and T. S. Rappaport, "Wideband measurements of angle and delay dispersion for outdoor and indoor peer-to-peer radio channels at 1920 MHz," *IEEE Trans. Antennas Propagat.*, vol. 51, pp. 936–944, May 2003.

[91] R. Kattenbach, "Statistical modeling of small-scale fading in directional radio channels," *IEEE J. Sel. Areas Commun.*, vol. 20, pp. 584–592, Apr. 2002.

[92] R. J. M. Cramer, R. A. Scholtz, and M. M. Z. Win, "Evaluation of an ultra-wide-band propagation channel," *IEEE Trans. Antennas Propagat.*, vol. 50, pp. 561–570, May 2002.

[93] A. Kuchar, J. P. Rossi, and E. Bonek, "Directional macro-cell channel characterization from urban measurements," *IEEE Trans. Antennas Propagat.*, vol. 48, pp. 137–146, Feb. 2000.

[94] F. Harryson, J. Medbo, A. F. Molisch, F. Tufvesson, and A. J. Johansson, "The composite channel method: Efficient experimental evaluation of

realistic MIMO terminal in the presence of human body," in *Proc. IEEE VTC*, 2008.

[95] A. F. Molisch and H. Hofstetter, "The COST 273 MIMO channel model," in *Mobile Broadband Multimedia Networks*, L. Correia, Ed. New York: Academic, 2006.

[96] J. Fuhl, A. F. Molisch, and E. Bonek, "Unified channel model for mobile radio systems with smart antennas," *Proc. Inst. Elect. Eng. Radar, Sonar Navig.*, vol. 145, pp. 32–41, 1998.

[97] M. Steinbauer and A. F. Molisch, "Directional channel models," in *Flexible Personalized Wireless Communications*, ch. 3.2, L. Correia, Ed. New York: Wiley, 2001.

[98] A. Saleh and R. A. Valenzuela, "A statistical model for indoor multipath propagation," *IEEE J. Sel. Areas Commun.*, vol. SAC-5, pp. 128–137, Feb. 1987.

[99] A. F. Molisch, A. Kuchar, J. Laurila, K. Hugl, and R. Schmalenberger, "Geometry-based directional model for mobile radio channels-principles and implementation," *Eur. Trans. Telecommun.*, vol. 14, pp. 351–359, 2003.

[100] A. F. Molisch, "A generic model for MIMO wireless propagation channels in macro- and microcells," *IEEE Trans. Signal Process.*, vol. 52, pp. 61–71, Jan. 2004.

[101] V. Erceg *et al.*, "Indoor MIMO WLAN channel models," IEEE 802.11 Standardization Draft, 2003.

[102] M. Nilsson, B. Lindmark, M. Ahlberg, M. Larsson, and C. Beckman, "Measurements of the spatio-temporal polarization characteristics of a radio channel at 1800 MHz," in *Proc. IEEE Veh. Technol. Conf.*, 1999, pp. 386–391.

[103] P. Soma, D. S. Baum, V. Erceg, R. Krishnamoorthy, and A. J. Paulraj, "Analysis and modeling of multiple-input multiple-output (MIMO) radio channel based on outdoor measurements conducted at 2.5 GHz for fixed BWA applications," in *Proc. IEEE Int. Conf. Commun.*, 2002, pp. 272–276.

[104] ITU-R, Guidelines for evaluation of radio transmission technologies for IMT-2000, Rec. ITU-R M.1225, 1997.

[105] ITU, "Method for point-to-area predictions for terrestrial services in the frequency range 30 MHz to 3000 MHz," Rec. ITU P 1546-3, 2007.

[106] Commission of the European Communities, "Digital land mobile radio communications," Final Rep. COST 207.

[107] "Spatial channel model for multiple input multiple output (MIMO) simulations (Rel. 7)," 3GPP TR 25.996 V7.0.0, 2007.

[108] G. Calcev, D. Chizhik, B. Goransson, S. Howard, H. Huang, A. Kogiantis, A. F. Molisch, A. L. Moustakas, D. Reed, and H. Xu, "A wideband spatial channel model for system-wide simulations," *IEEE Trans. Veh. Technol.*, vol. 56, pp. 389–403, 2007.

[109] J. Medbo and P. Schramm, "Channel models for HIPERLAN/2," ETSI/BRAN Doc. 3ERI085B.

[110] *Delay Dispersion in UWB Residential/Office Environments*, IEEE 802.15.3a.

[111] A. F. Molisch, J. R. Foerster, and M. Pendergrass, "Channel models for ultrawideband personal area networks," *IEEE Wireless Commun.*, vol. 10, pp. 14–21, Dec. 2003.

[112] *Delay Dispersion in UWB Channels (Office, Residential, Outdoor, Industrial)*, IEEE 802.15.4a.

[113] A. F. Molisch, K. Balakrishnan, C. C. Chong, D. Cassioli, S. Emami, A. Fort, J. Karedal, J. Kunisch, H. Schantz, K. Siwiak, and M. Z. Win, "A comprehensive model for ultrawideband propagation channels," *IEEE Trans. Antennas Propagat.*, pp. 3151–3166, 2006.

[114] V. Erceg *et al.*, "TGn channel models," IEEE 802.11-03/940r4.

## ABOUT THE AUTHORS

**Andreas F. Molisch** (Fellow, IEEE) received the Dipl. Ing., Dr. Techn., and Habilitation degrees from Technical University (TU) Vienna, Austria, in 1990, 1994, and 1999, respectively.

From 1991 to 2000, he was with TU Vienna, becoming an Associate Professor there in 1999. From 2000 to 2002, he was with the Wireless Systems Research Department, AT&T (Bell) Laboratories Research, Middletown, NJ. From 2002–2008, he was with Mitsubishi Electric Research Labs, Cambridge, MA, most recently as Distinguished Member of Technical Staff and Chief Wireless Standards Architect, as well as Professor and Chairholder for radio systems at Lund University, Sweden. Since 2009, he is Professor of Electrical Engineering at the University of Southern California, Los Angeles, CA. His current research interests are measurement and modeling of mobile radio channels, UWB, cooperative communications, and MIMO systems. He has authored, coauthored or edited four books [among them *Wireless Communications* (New York: Wiley-IEEE Press)], 11 book chapters, some 110 journal papers, more than 180 conference papers, and more than 70 patents. He has been a member of numerous Technical Program Committees (TPCs) and TPC Chair or General Chair of several conferences. He has chaired, or been active in, a variety of international standards organizations.

Dr. Molisch is a Fellow of IEEE and IET. He is an Editor of the IEEE TRANSACTIONS ON WIRELESS COMMUNICATIONS. He was a Coeditor of recent special issues on UWB in the IEEE JOURNAL ON SELECTED AREAS IN COMMUNICATIONS and PROCEEDINGS OF THE IEEE. He is an IEEE Distinguished Lecturer and recipient of several awards.

**Larry J. Greenstein** (Life Fellow, IEEE) received the B.S., M.S., and Ph.D. degrees in electrical engineering from Illinois Institute of Technology (IIT), Chicago, in 1958, 1961, and 1967, respectively.

From 1958 to 1970, he was with IIT Research Institute, Chicago, working on radio-frequency interference and anticlutter airborne radar. He joined Bell Laboratories, Holmdel, NJ, in 1970. Over a 32-year AT&T career, he conducted research in digital communications satellites, point-to-point digital radio, optical fiber systems, and wireless communications. For 21 years during that period (1979–2000), he led a research department renowned for its contributions in these fields. He is now a Research Scientist with Rutgers-WINLAB, North Brunswick, NJ, working in the areas of ultra-wide-band systems, sensor networks, MIMO-based wireless systems, broadband power line systems, and radio channel modeling.

Dr. Greenstein is an AT&T Fellow. He received the IEEE Communications Society's Edwin Howard Armstrong Award and four Best Paper awards. He is currently Director of Journals for the IEEE Communications Society.

**Mansoor Shafi** (Fellow, IEEE) received the B.Sc. (Engineering) degree in electrical engineering from Engineering University, Lahore, Pakistan, in 1970 and the Ph.D. degree from the University of Auckland, Auckland, New Zealand, in 1979.

From 1975 to 1979, he was a Junior Lecturer at the University of Auckland. Since 1979, he has been with Telecom New Zealand, where he now is Principal Advisor Wireless Systems. His role is to advise Telecom management on the future directions of wireless technologies and standards. His research interests are in wireless communications. He is an Adjunct Professor at Canterbury University, U.K. He was a Cochair of the ICC 2005 Wireless Communications Symposium, Seoul, Korea. He serves as New Zealand delegate to meetings of the ITU-R.

Dr. Shafi was a Guest Editor of the IEEE JOURNAL ON SELECTED AREAS IN COMMUNICATIONS special issue on MIMO systems (April 2003). He was a corecipient of the IEEE Communications Society Best Tutorial Paper Award in 2004. He is an Editor of the IEEE TRANSACTIONS ON WIRELESS COMMUNICATIONS. He has published widely in IEEE JOURNALS and IEEE conferences in the areas of radio propagation, signal processing, MIMO systems, and adaptive equalization.